

Partial-wave analysis of $\vec{p}\vec{p} \rightarrow pp\pi^0$ data

P. N. Deepak, J. Haidenbauer, and C. Hanhart

Institut für Kernphysik (Theorie), Forschungszentrum Jülich

52428 Jülich, Germany

Abstract

We present a partial-wave analysis of the polarization data for the reaction $\vec{p}\vec{p} \rightarrow pp\pi^0$, based solely on the recent measurements at IUCF for this channel. The fit leads to a χ^2 per degree of freedom of 1.7. Methods for an improved analysis are discussed. We compare the extracted values to those from a meson exchange model.

1 Introduction

Understanding pion production in nucleon-nucleon (NN) collisions near threshold is of high theoretical interest for various reasons. As the first strong inelasticity for the NN system, its phenomenology is closely linked to that of elastic NN scattering (for recent reviews on the subject of near-threshold pion production see Refs. [1, 2]). In addition, as the pion is a Goldstone-boson of the chiral symmetry of strong interactions, its dynamics is strongly constrained by this symmetry (see Ref. [3] and references therein). Recently a scheme was discussed that is said to lead to a convergent effective field theory even for large momentum transfer reactions such as $NN \rightarrow NN\pi$ [4, 5]. Confirmation of this claim is the precondition for a successful analysis of the isospin violating pion production reactions measured recently, namely the forward-backward asymmetry in $pn \rightarrow d\pi^0$ [6] and the total cross section measurement for $dd \rightarrow \alpha\pi^0$ [7].

A complete set of polarization observables for the reaction $\vec{p}\vec{p} \rightarrow pp\pi^0$ was measured for the first time in 2001 [8]. Of the two existing advanced models of pion production in NN collisions [9, 10] that include higher partial waves and therefore allow predictions for polarization observables, only the model of the Jülich group [9, 11] has been thoroughly confronted with those data. Thereby it turned out that this model failed to provide an overall satisfactory reproduction of these polarization observables [8, 12]. On the other hand, the (less complete) data for $\vec{p}\vec{p} \rightarrow pn\pi^+$ [13] as well as those for $\vec{p}\vec{p} \rightarrow d\pi^+$ [14] were described very well by the same model. So far the reason(s) for the short-coming of this phenomenological model to describe the neutral pion production – while being rather successful for the charged pions – is not yet understood¹.

¹Note, however, that effective field theory studies revealed many conceptual problems in this approach, as discussed in [2]; it is up to now unclear how much impact those have on the description of the observables.

No.	Type	Our notation $T_{l_q(L_p s_f)j; L s_i}^J$	Notation of Meyer et al. [8] ${}^{2s_i+1}L_J \rightarrow {}^{2s_f+1}L_{pj}, l_q$
1	Ss	$T_{0(00)0;11}^0$	${}^3P_0 \rightarrow {}^1S_0, s$
2	Ps	$T_{0(11)0;00}^0$	${}^1S_0 \rightarrow {}^3P_0, s$
3		$T_{0(11)2;20}^2$	${}^1D_2 \rightarrow {}^3P_2, s$
4	Pp	$T_{1(11)1;11}^0$	${}^3P_0 \rightarrow {}^3P_1, p$
5		$T_{1(11)1;11}^2$	${}^3P_2 \rightarrow {}^3P_1, p$
6		$T_{1(11)2;11}^2$	${}^3P_2 \rightarrow {}^3P_2, p$
7		$T_{1(11)1;31}^2$	${}^3F_2 \rightarrow {}^3P_1, p$
8		$T_{1(11)2;31}^2$	${}^3F_2 \rightarrow {}^3P_2, p$
9		$T_{1(11)0;11}^1$	${}^3P_1 \rightarrow {}^3P_0, p$
10		$T_{1(11)1;11}^1$	${}^3P_1 \rightarrow {}^3P_1, p$
11		$T_{1(11)2;11}^1$	${}^3P_1 \rightarrow {}^3P_2, p$
12		$T_{1(11)2;31}^3$	${}^3F_3 \rightarrow {}^3P_2, p$
13	Sd	$T_{2(00)0;11}^2$	${}^3P_2 \rightarrow {}^1S_0, d$
14		$T_{2(00)0;31}^2$	${}^3F_2 \rightarrow {}^1S_0, d$
15	Ds	$T_{0(20)2;11}^2$	${}^3P_2 \rightarrow {}^1D_2, s$
16		$T_{0(20)2;31}^2$	${}^3F_2 \rightarrow {}^1D_2, s$

Table 1: Partial-wave amplitudes that could contribute to $\vec{p}\vec{p} \rightarrow pp\pi^0$ near threshold. Only contributions arising from the first 12 amplitudes were considered in the present analysis.

The presence of spin leads to contributions of many partial-wave amplitudes, even close to threshold, which is the regime of interest here. It is thus difficult to draw any more concrete conclusion from a comparison of the model results directly with the data. It is well known that a partial-wave analysis is an important intermediate step towards an understanding of hadronic reactions: being in principle equivalent to the full data set, the partial-wave amplitudes can be much more easily interpreted in terms of their physics content. As a consequence, a comparison of the theoretical results with the partial-wave amplitudes is expected to reveal the strengths/weaknesses of the theory much more clearly than a direct comparison with the data.

In this paper we present a first step towards a full partial-wave decomposition of the reaction $pp \rightarrow pp\pi^0$. In our work we use as input only data from the recent IUCF measurement [8]. However, as will be stressed below, a combined analysis of both the production data and the data on elastic scattering is mandatory for the future. In [8], the various angular-dependent structures of the polarization observables were fitted under particular assumptions on the partial wave content of the data as well as on the energy dependence of some of the amplitudes. These assumptions were necessitated by the limited statistical accuracy of the data. As we use the extracted coefficients of Ref. [8] as input for our fitting procedure, we also have to make the same assumptions in our analysis.

This paper is organized as follows: in the next section we will describe the theoretical formalism that allows to relate the observables to the partial-wave amplitudes. In section 3 the

method of extraction as well as that for determining the uncertainties are explained. Then, in section 4 we discuss the results and compare them to those of a microscopic model [9]. The paper closes with a short summary and a discussion of further steps.

2 Theoretical formalism

The T -matrix for $pp \rightarrow pp\pi^0$ may be expressed in the form [15]

$$T = \sum_{s_f, s_i=0}^1 \sum_{\lambda=|s_i-s_f|}^{s_i+s_f} (S^\lambda(s_f, s_i) \cdot T^\lambda(s_f, s_i)), \quad (1)$$

where s_i, s_f denote the initial and final channel-spins respectively. We use the same notations as in [16], where the irreducible channel-spin transition operators $S_{m_\lambda}^\lambda(s_f, s_i)$ of rank λ are defined. If in c.m., \vec{p}_i, \vec{p} denote the relative momenta of the two protons in the initial and final states and \vec{q} the momentum of the pion, the irreducible tensor reaction-amplitudes $T_{m_\lambda}^\lambda(s_f, s_i)$ in (1) can be expressed in the form [15]

$$\begin{aligned} T_{m_\lambda}^\lambda(s_f, s_i) = & \sum_{L_p, L, l_q} \sum_{j, J, L_f} (-1)^{L_f} [j][L_f][J]^2 [s_f]^{-1} \begin{Bmatrix} s_f & L_f & J \\ L & s_i & \lambda \end{Bmatrix} \begin{Bmatrix} s_f & L_p & j \\ l_q & J & L_f \end{Bmatrix} \\ & \times T_{l_q(L_p s_f)j; L s_i}^J ((Y_{L_p}(\hat{p}) \otimes Y_{l_q}(\hat{q}))^{L_f} \otimes Y_L(\hat{p}_i))_{m_\lambda}^\lambda \end{aligned} \quad (2)$$

to separate the energy and angular dependence of the amplitudes. In Eq. (2), we use the short-hand notation $[j] = \sqrt{2j+1}$ and $(T_1 \otimes T_2)_m^L$ indicates the coupling of the two irreducible tensors T_1 and T_2 to total angular momentum L with projection m . The partial-wave amplitudes $T_{l_q(L_p s_f)j; L s_i}^J$ are functions of both the c.m. energy E_{cm} and ϵ , the relative kinetic energy of the nucleon pair in the final state (in contrast to a two body reaction, where the partial-wave amplitudes are characterized by a single energy variable).

If \vec{P}, \vec{Q} denote respectively the beam and target polarizations, the differential cross section in a double-polarized experiment may be written as [15]

$$\frac{d\sigma}{d\Omega_p d\Omega_q d\epsilon} = \frac{1}{4} \sum_{k_1, k_2=0}^1 \sum_{k=|k_1-k_2|}^{k_1+k_2} ((P^{k_1} \otimes Q^{k_2})^k \cdot B^k(k_1, k_2)), \quad (3)$$

in terms of the irreducible tensors

$$\begin{aligned} B_\nu^k(k_1, k_2) = & 2(-1)^{k_1+k_2} [k_1][k_2] \sum_{s_f=0}^1 (2s_f+1) \sum_{s_i, s'_i=0}^1 \sum_{\lambda, \lambda'} (-1)^{s'_i+s_f} [s_i][s'_i][\lambda][\lambda'] \\ & \times \begin{Bmatrix} s'_i & s_i & k \\ \lambda & \lambda' & s_f \end{Bmatrix} \begin{Bmatrix} \frac{1}{2} & \frac{1}{2} & s_i \\ \frac{1}{2} & \frac{1}{2} & s'_i \\ k_1 & k_2 & k \end{Bmatrix} (T^\lambda(s_f, s_i) \otimes T^{\lambda'}(s_f, s'_i))_\nu^k, \end{aligned} \quad (4)$$

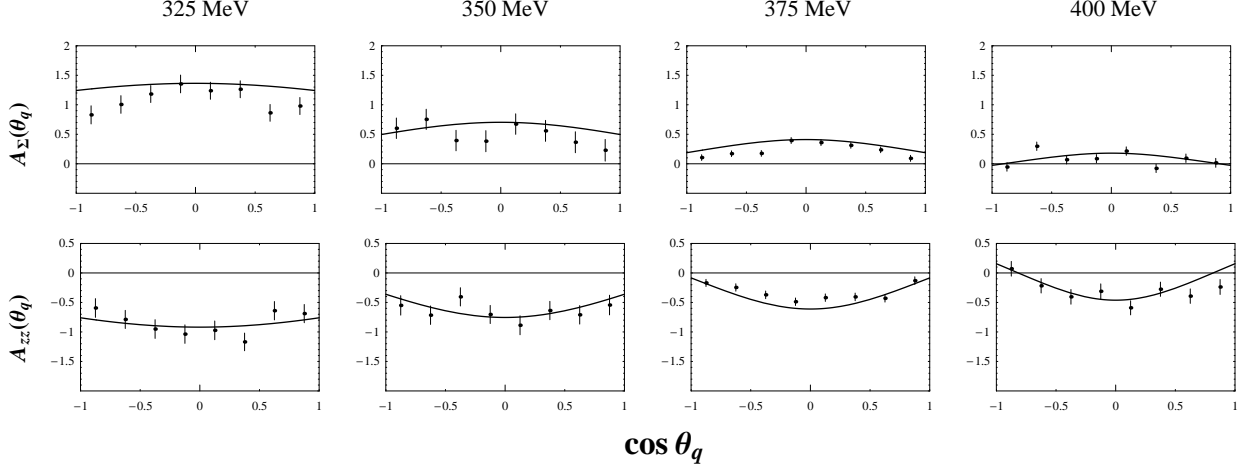


Figure 1: The observables $A_{\Sigma}(\theta_q)$ and $A_{zz}(\theta_q)$ as a function of the pion angle at several bombarding energies. The data and the nomenclature for the observables are taken from Meyer et al. [8]. The solid lines represent our results.

which are bilinear in the irreducible tensor amplitudes $T_{m\lambda}^{\lambda}(s_f, s_i)$ whose complex conjugates $T_{m\lambda}^{\lambda}(s_f, s_i)^*$ define $T_{m\lambda}^{\dagger\lambda}(s_f, s_i) = (-1)^{m\lambda} T_{-m\lambda}^{\lambda}(s_f, s_i)^*$. If

$$\sigma_0(\xi) = \frac{1}{4} B_0^0(0, 0) \quad (5)$$

denotes the unpolarized differential cross section with ξ collectively standing for $\{\hat{p}, \hat{q}, \epsilon\}$, the $B_{\nu}^k(k_1, k_2)$ are related to the independent (Cartesian) spin-observables $A_{ij}(\xi)$, defined in [8], through

$$\sigma_0(\xi) A_{y0}(\xi) = \frac{-1}{2\sqrt{2}} \Im(B_1^1(1, 0)); \quad (6a)$$

$$\sigma_0(\xi) A_{xz}(\xi) = \frac{1}{4} [\Re(B_1^1(1, 1) - B_1^2(1, 1))]; \quad (6b)$$

$$\sigma_0(\xi) A_{\Sigma}(\xi) = \frac{-1}{2\sqrt{3}} [B_0^0(1, 1) + \frac{1}{\sqrt{2}} B_0^2(1, 1)]; \quad (6c)$$

$$\sigma_0(\xi) A_{zz}(\xi) = \frac{-1}{4\sqrt{3}} [B_0^0(1, 1) - \sqrt{2} B_0^2(1, 1)]; \quad (6d)$$

$$\sigma_0(\xi) A_{\Delta}(\xi) = \frac{1}{2} \Re(B_2^2(1, 1)); \quad (6e)$$

$$\sigma_0(\xi) A_{z0}(\xi) = \frac{1}{4} B_0^1(1, 0); \quad (6f)$$

$$\sigma_0(\xi) A_{\Xi}(\xi) = \frac{-1}{2\sqrt{2}} \Im(B_0^1(1, 1)). \quad (6g)$$

3 Extraction of partial-wave amplitudes

A priori, a set of 16 partial-wave amplitudes can be expected to contribute to the reaction. We list them in Table 1, explicitly both in our notation and the notation of Meyer et al. [8]. But we consider only contributions from the first 12 amplitudes since final states with orbital angular momentum greater than 1 were ignored in the analysis of Meyer et al. [8]. Thus there

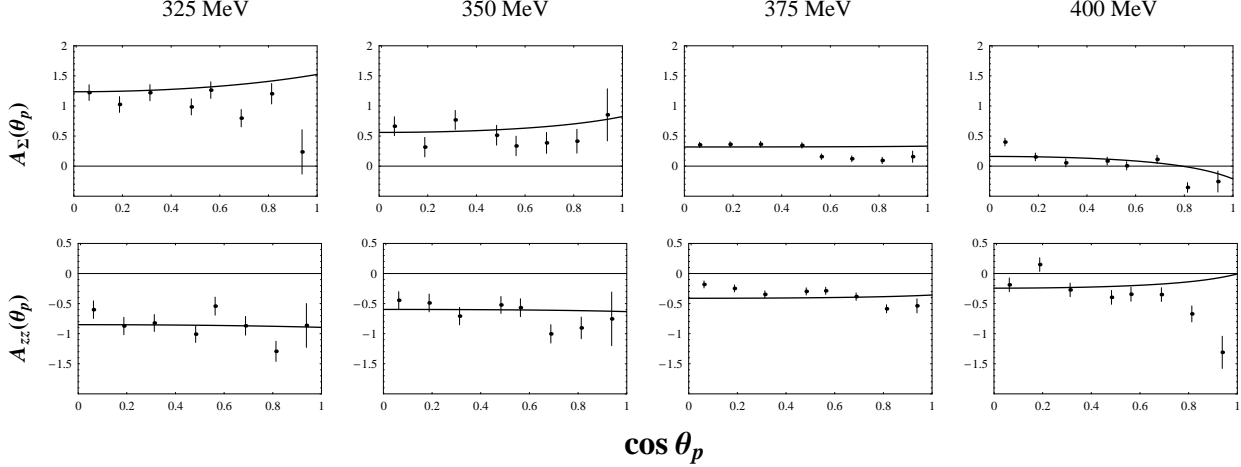


Figure 2: The observables $A_{\Sigma}(\theta_p)$ and $A_{zz}(\theta_p)$ as a function of the proton angle at several bombarding energies.

are 24 real unknowns (12 complex amplitudes) to be determined. However, as overall phases are unobservable and $s_f = 0$ and $s_f = 1$ NN -final-states do not mix with each other in any of the spin-observables measured in [8] (final state polarizations were not measured), we have the freedom to choose the first two amplitudes to be real. This leaves 22 real numbers to be determined. Equations (11a)-(11h) of [8] represent the general angular dependence of $\sigma_0(\xi)$ and $\sigma_0(\xi)A_{ij}(\xi)$ in terms of the real coefficients E , F_k , G_k^{ij} , H_k^{ij} , I , K , I^{ij} and K^{ij} . The quantities E , F_k , G_k^{ij} and H_k^{ij} denote the weighted sums of bilinears in the partial-wave amplitudes corresponding respectively to $(Ss)^2$, $(Ps)^2$, $(PsPp)$ and $(Pp)^2$ interference terms, while I , I^{ij} and K , K^{ij} represent respectively the contribution of $(SsSd)$ and $(SsDs)$ interference terms, which were ignored in the analysis of [8] and therefore also here. Using Eqs. (4) and (2), we obtain explicit expressions for all the observables in (6a)-(6g) including the unpolarized differential cross section, defined in (5), in terms of the first 12 partial-wave amplitudes listed in Table 1. These expressions when compared with Eqs. (11a)-(11h) of [8], allow us to obtain explicitly the partial-wave decomposition of the coefficients E , F_k , G_k^{ij} and H_k^{ij} .

Note that all values given in Table IV of [8] for the various coefficients are integrated with respect to the outgoing two nucleon energy, ϵ . Thus, they are expressed as weighted sums of numerous $\mathcal{B}_{\kappa\kappa'}$, bilinear in the partial-wave amplitudes, as (we use non-relativistic kinematics)

$$\mathcal{B}_{\kappa\kappa'}(E_{\text{cm}}) = \int_0^{\epsilon_{\text{max}}} T_{\kappa}(E_{\text{cm}}, \epsilon) T_{\kappa'}^*(E_{\text{cm}}, \epsilon) q(E_{\text{cm}}, \epsilon) p(\epsilon) d\epsilon, \quad (7)$$

where T_{κ} , $\kappa = 2, \dots, 12$, denotes the κ^{th} partial-wave amplitude listed in Table 1 (for example, $T_5(E_{\text{cm}}, \epsilon) \equiv T_{1(11)1;11}^2$), $p(\epsilon) = \sqrt{M_N \epsilon}$ and $q(E_{\text{cm}}, \epsilon) = \sqrt{2\mu(E_{\text{cm}} - 2M_N - m_{\pi} - \epsilon)}$, with the reduced mass of the outgoing three body system $\mu = 2m_{\pi}M_N/(m_{\pi} + 2M_N)$, where M_N and m_{π} are the nucleon and pion masses, respectively. Thus, to proceed further we need to make an assumption regarding the ϵ -dependence of the T_{κ} . In the present first analysis of the IUCF data we use the most naive ansatz possible: we assume that the entire energy dependence of the amplitudes stems solely from the centrifugal barrier. This gives

$$T_{\kappa}(E_{\text{cm}}, \epsilon) \propto q(E_{\text{cm}}, \epsilon)^{l_q(\kappa)} p(\epsilon)^{L_p(\kappa)}, \quad (8)$$

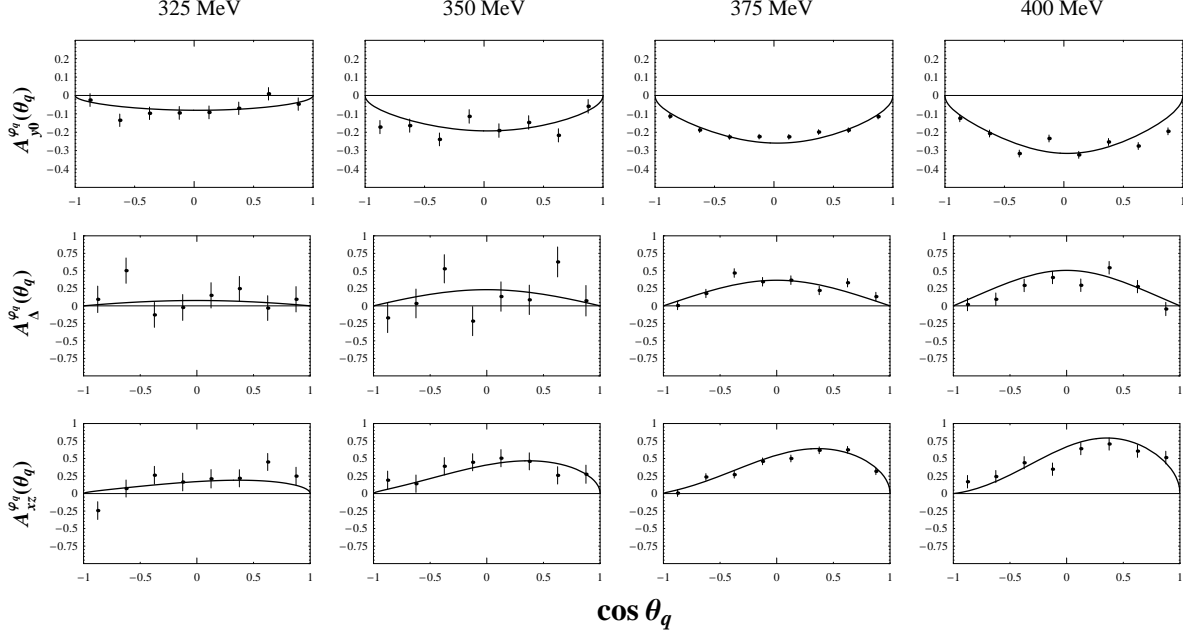


Figure 3: The observables $A_{y0}^{\varphi_q}(\theta_q)$, $A_{xz}^{\varphi_q}(\theta_q)$ and $A_{\Delta}^{\varphi_q}(\theta_q)$ as a function of the pion angle at several bombarding energies.

which should hold as long as the outgoing momenta are small compared to the inverse of the production radius [18] and the effects of the final state interaction (FSI) are negligible. (This is obviously wrong for the NN S -waves; they are discussed separately below.) Note, the same assumption was also used in the fitting procedure of Ref. [8] in order to determine some of the coefficients E , F_k , G_k^{ij} and H_k^{ij} from the data, for the statistical accuracy of the data did not allow for a separate fit of these coefficients at each energy. From the ansatz of Eq. (8), one easily derives

$$\mathcal{B}_{\kappa\kappa'}(E_{\text{cm}}) = z_{\kappa} z_{\kappa'}^* \eta^{l_q(\kappa)+l_q(\kappa')+L_p(\kappa)+L_p(\kappa')+4} . \quad (9)$$

Thus, we find the energy dependence of the $\mathcal{B}_{\kappa\kappa'}$, $\kappa, \kappa' = 2, \dots, 12$, to be of the form η^x , with x equal to 6, 7 and 8 for the PsPs, PsPp and PpPp interference terms, respectively. Here $\eta = q_{\text{max}}/m_{\pi}$ with q_{max} being the largest possible value of pion momentum for a given incident energy. By assumption, z_{κ} , $\kappa = 2, \dots, 12$ in (9) are energy-independent complex quantities to be determined from the data.

Since the transition amplitude with the Ss final-state does not interfere with any of the other partial waves and since its FSI does not show a power law behavior [19], we parameterize it as

$$\mathcal{B}_{11}(E_{\text{cm}}) = \int_0^{\epsilon_{\text{max}}} |T_1(E_{\text{cm}}, \epsilon)|^2 q(E_{\text{cm}}, \epsilon) p(\epsilon) d\epsilon = |z_1|^2 \quad (10)$$

and extract it at each of the four bombarding energies individually; $\mathcal{B}_{11}(E_{\text{cm}})$ is directly proportional to the bilinear coefficient E in Table IV of Ref. [8].

The values of the coefficients H_1^{00} , H_1^{zz} , F_2 , H_2^{Σ} , H_2^{zz} , G_1^{z0} , G_1^{Ξ} , H_1^{z0} , H_2^{z0} , H_4^{Σ} , H_5^{Σ} , H_4^{zz} and H_5^{zz} were determined by Meyer et al. [8] by assuming their energy dependence to be of the form

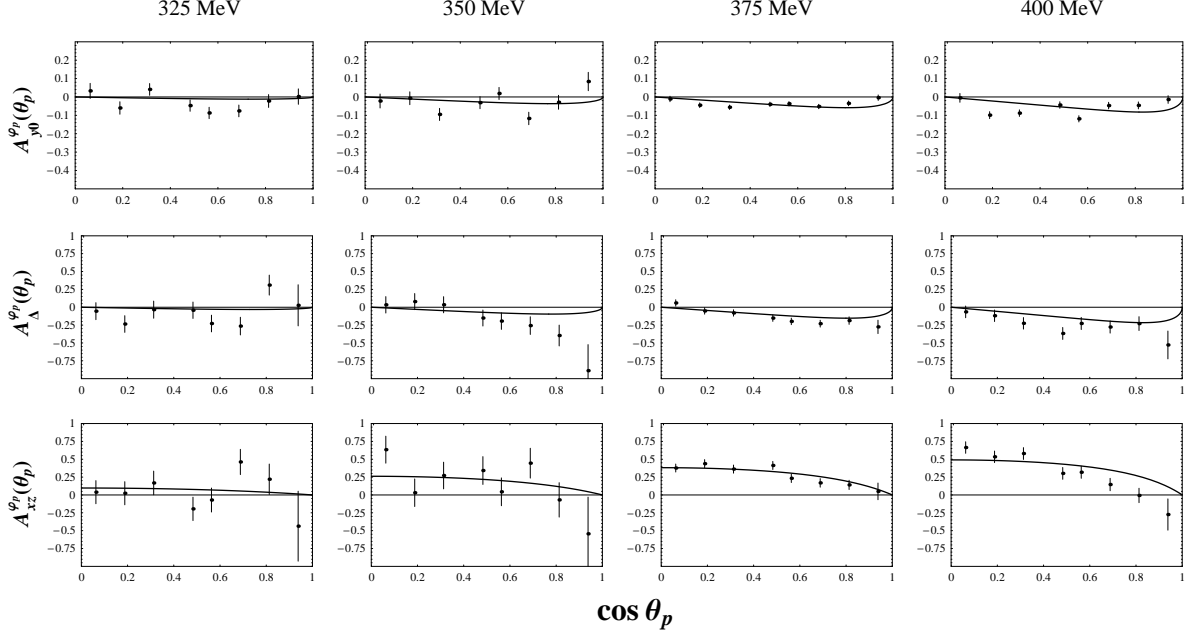


Figure 4: The observables $A_{y0}^{\varphi_p}(\theta_p)$, $A_{xz}^{\varphi_p}(\theta_p)$ and $A_{\Delta}^{\varphi_p}(\theta_p)$ as a function of the proton angle at several bombarding energies.

given in Eq. (9). Therefore, in order to be consistent with [8], we do the following. We plot each of these 13 coefficients as a function of their appropriate η -dependence and extract the slope and the corresponding error, using the values and errors in Table IV of [8]. For example, $(\sigma_{tot}(\eta)F_2(\eta))/(8\pi^2)$ is plotted against η^6 . The values and errors so obtained were then used in our fitting procedure. This gives us a set of 13 equations for the amplitudes z_{κ} , $\kappa = 2, \dots, 12$. The remaining 26 coefficients, viz., F_1 , H_0^{Σ} , H_0^{zz} and the 23 coefficients from G_1^{y0} to H_5^{Δ} , in Table IV of [8] lead to $26 \times 4 = 104$ equations for the amplitudes z_{κ} , $\kappa = 2, \dots, 12$, as they were extracted by [8] without any assumption about their energy dependence. Both the values and errors for these 104 coefficients, taken from Table IV of [8], were multiplied by $(\sigma_{tot}(\eta)/(8\pi^2))$ for consistency. In total, we have 117 equations with 21 real unknowns (since z_2 is assumed to be real). In addition, the coefficient E depends only on z_1 . Since this amplitude is assumed to be real and we know the explicit dependence of E on z_1 , it is directly determined (up to a sign). The uncertainty in z_1 , is determined by that in E .

This nonlinear overdetermined system of 117 equations can only have approximate solutions, which were obtained by χ^2 -minimization using the software *Mathematica*. The resulting χ^2 per degree of freedom was 1.7. This value was the best that we could obtain after using all the four methods of minimization available with *Mathematica*, viz., differential evolution, Nelder-Mead, random search and simulated annealing. We performed various checks (different starting vectors; setting individual amplitudes to zero) to further support that the minimum is indeed a total minimum. In Figs. 1-6, to illustrate the quality of the fit, we compare our results to some of the observables measured in [8].

The uncertainties in the z_{κ} , $\kappa = 2, \dots, 12$, were determined as follows. Let \mathbf{a} denote the vector whose 21 components are the real and imaginary parts of the amplitudes z_i . Then the

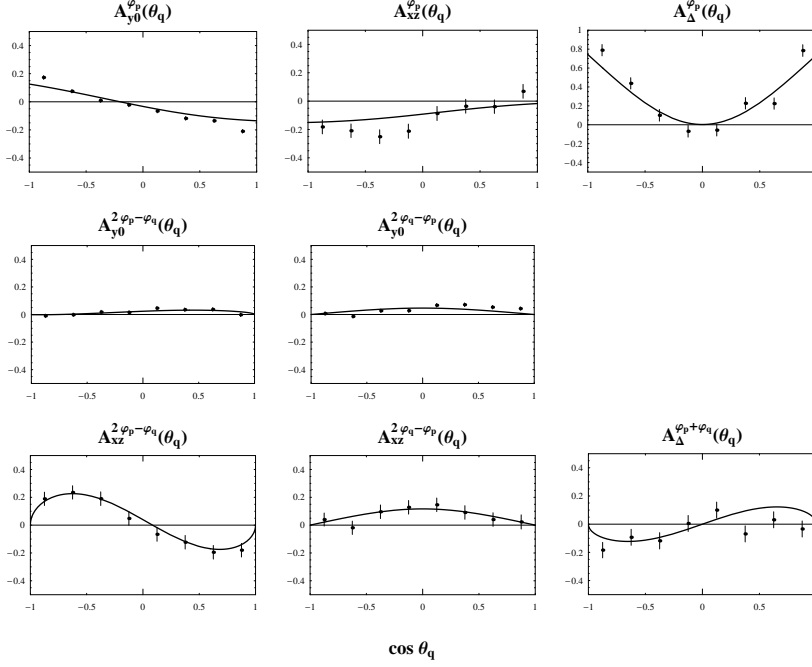


Figure 5: Additional observables at a bombarding energy of 375 MeV as a function of the pion angle.

uncertainty (standard deviation) in any of the components, say a_j , denoted by σ_{a_j} , is obtained through [20]

$$\sigma_{a_j}^2 = \sum_{i=1}^{117} \left(\sum_{l=1}^{21} \frac{1}{\sigma_i} \left(\epsilon_{jl} \frac{\partial}{\partial a_l} f_i(\mathbf{a}) \right)_{\mathbf{a}=\mathbf{a}_0} \right)^2. \quad (11)$$

Here $f_i(\mathbf{a})$ stands for the explicit functional form of the bilinear coefficients listed in Table IV of [8], in terms of the z_κ . σ_i are the corresponding errors in these bilinear coefficients, taken from the same Table and ϵ_{jl} is the (j, l) -th element of the error (covariance) matrix ϵ defined as the inverse of the curvature matrix α whose elements are given by

$$\alpha_{jl} \equiv \frac{1}{2} \frac{\partial^2 \chi^2}{\partial a_j \partial a_l}. \quad (12)$$

Here \mathbf{a}_0 is the value of \mathbf{a} for which the value of χ^2 is at its minimum.

4 Results and discussion

In Figs. 7-8, the values for the z_κ , $\kappa = 1, \dots, 12$, as determined in the fit are plotted. The uncertainties quoted in these figures for $|z_\kappa|$, $\kappa = 1, \dots, 12$ and $\tan(\text{Arg}(z_\kappa))$, $\kappa = 3, \dots, 12$, were determined by propagating the errors obtained for the real and imaginary parts of the z_κ , $\kappa = 1, \dots, 12$, in the standard way [21]. It is striking that the amplitude z_2 , corresponding to the transition $^1S_0 \rightarrow ^3P_0s$, is the largest.

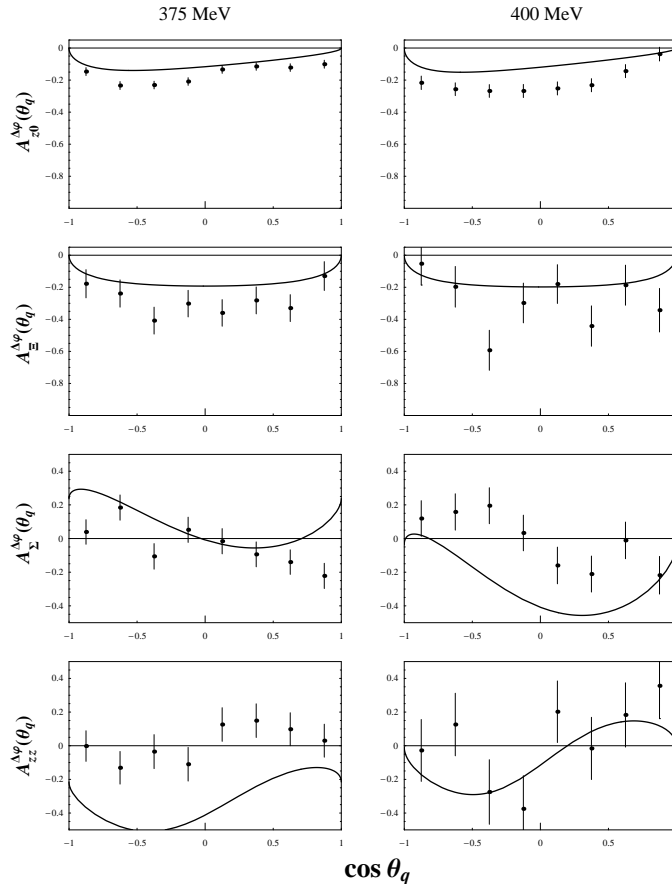


Figure 6: Observables that depend on $\Delta\varphi_q$, plotted as a function of the angle θ_q at the bombarding energies of 375 and 400 MeV, at which the measurement of Ref. [8] has the best statistics.

We now turn to a comparison of the extracted z_κ with the predictions of the microscopic model of the Jülich group. For a detailed description of the model we refer the reader to Refs. [9, 12]. Here we only want to summarize its salient features. In the Jülich model all standard pion-production mechanisms (direct production (Fig. 9a), pion rescattering (Fig. 9b), contributions from pair diagrams (Fig. 9c)) are considered. In addition, production mechanisms involving the excitation of the $\Delta(1232)$ resonance (cf. Fig. 9d–g) are taken into account explicitly. All NN partial waves up to orbital angular momenta $L_p = 2$, and all states with relative orbital angular momentum $l_q \leq 2$ between the NN system and the pion are considered in the final state. Furthermore all πN partial waves up to orbital angular momenta $L_{\pi N} = 1$ are included in calculating the rescattering diagrams in Fig. 9b,e and g. Thus, this model includes not only s-wave pion rescattering but also contributions from p-wave rescattering.

The reaction $NN \rightarrow NN\pi$ is treated in a distorted wave born approximation, in the standard fashion. The actual calculations are carried out in momentum space. For the distortions in the initial and final NN states, a coupled channel ($NN, N\Delta, \Delta\Delta$) model is employed [22] that treats the nucleon and the Δ degrees of freedom on equal footing. Thus, the $NN \leftrightarrow N\Delta$ transition amplitudes and the NN T-matrices that enter in the evaluation of the pion pro-

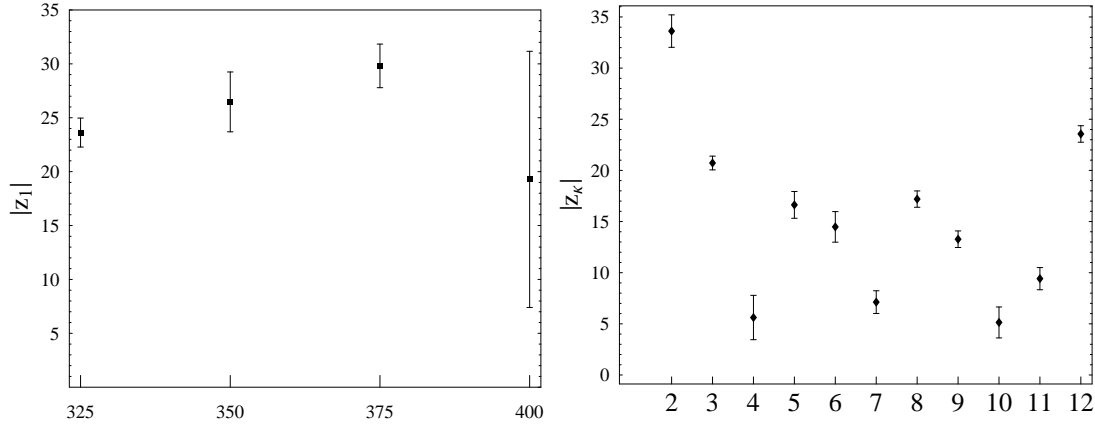


Figure 7: Left panel: Moduli (in $(\mu\text{b})^{1/2}$) of z_1 for bombarding energies of 325, 350, 375, and 400 MeV. Right panel: Moduli (in $(\mu\text{b})^{1/2}$) of the z_κ , $\kappa = 2, \dots, 12$.

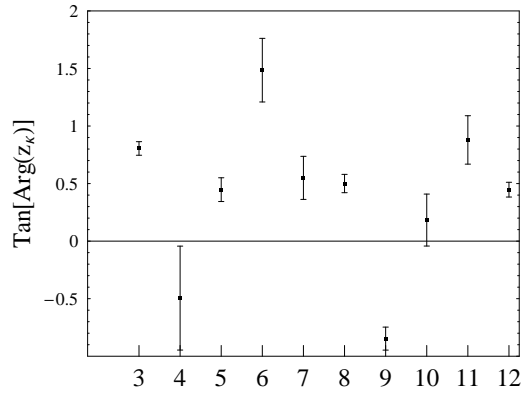


Figure 8: Tangent of the arguments of the z_κ , $\kappa = 3, \dots, 12$.

duction diagrams in Fig. 9 are consistent solutions of the same (coupled-channel) Lippmann–Schwinger-like equation.

By taking the partial-wave amplitudes $T_\kappa(E_{\text{cm}}, \epsilon)$ predicted by the model, it is straightforward to extract the moduli of the z_κ from the model through their definition in Eqs. (7) and (9):

$$|z_\kappa^{\text{model}}| = \eta^{-l_q(\kappa) - L_p(\kappa) - 2} \sqrt{\mathcal{B}_{\kappa\kappa}(E_{\text{cm}})} .$$

Since the phases of the bilinears $\mathcal{B}_{\kappa\kappa'}$ calculated from the model are not in all cases consistent with the factorization used in Eq. (9), they can not be compared easily with those extracted from the data.

The $|z_\kappa|$ predicted by the model are compared with the results of the partial-wave analysis in Fig. 10. In the upper part of the graph we compare the moduli of the z_κ of the model with those obtained by our partial-wave analysis, while in the lower part, the deviation of the model predictions from the analysis are presented. Note that the model results are normalized in such a way that $|z_1|$ for a bombarding energy of 375 MeV (i.e. the one corresponding to the

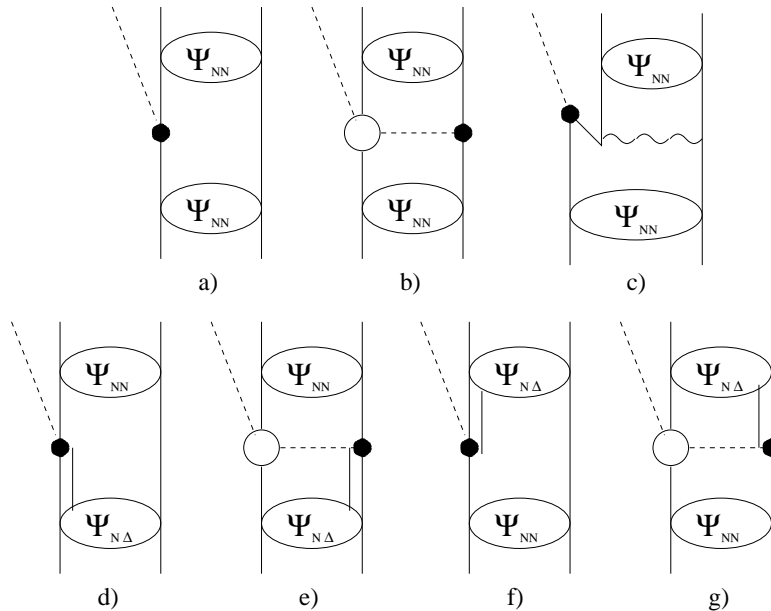


Figure 9: Pion production mechanisms taken into account in the model of Ref. [9]: (a) direct production; (b) pion rescattering; (c) contributions from pair diagrams; (d) to (g) production involving the excitation of the $\Delta(1232)$ resonance, depicted by the double line. In the diagrams the pion (nucleon) is shown as a dashed (solid) line.

$^3P_0 \rightarrow ^1S_0$ transition) coincides with the corresponding extracted value. This is done in order to facilitate the comparison between the various other $|z_\kappa|$.

It is evident from Fig. 10 that the microscopic model of Refs. [9, 12] yields a rather impressive overall description of the various partial-wave amplitudes, cf. the filled squares and circles. This is particularly remarkable because one has to keep in mind that practically all parameters of the model were fixed by other reactions (elastic- NN -scattering and πN scattering)². In fact the majority of the partial-wave amplitudes is reproduced even quantitatively (if one takes into account the error bars of the partial-wave analysis). The only serious discrepancy occurs in the amplitude z_9 ($^3P_1 \rightarrow ^3S_1p$) and to a lesser extent also in z_{12} ($^3F_3 \rightarrow ^3P_0p$). The reason for the short-coming in the model prediction for these $|z_\kappa|$ and the connection with its dynamical ingredients needs to be explored in the future.

Fig. 10 suggests also considerable deviations in z_{13} , z_{15} and especially in z_{16} . However, these z_κ correspond to partial waves with NN D -waves or pion d -waves in the final state whose contribution had been set to zero in the analysis of Meyer et al. [8]—as well as in ours—as already mentioned above. Thus, the predictions of the microscopic model can be seen as an indication that those amplitudes may not be negligible and therefore should be taken into account in any future analysis of the reaction $pp \rightarrow pp\pi^0$. Since in the present analysis, the neglected contributions of the D -wave and d -wave amplitudes are presumably mimicked by other partial-wave amplitudes, a more complete partial-wave analysis could yield results that are even closer to the model prediction than for the case considered in the present paper.

²The only free parameter was fixed to the total cross section for $pp \rightarrow pp\pi^0$ at low energies [11].

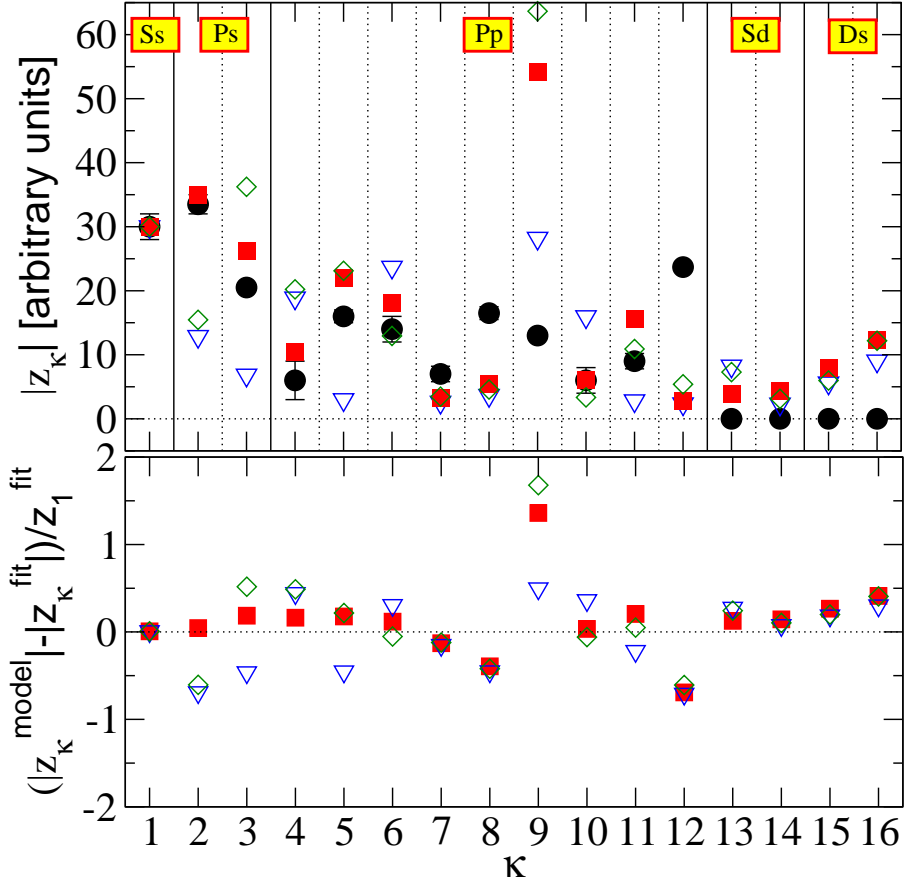


Figure 10: Comparison of the extracted $|z_\kappa|$ (filled circles) to the corresponding quantities predicted by the microscopic model of Ref. [9] (filled squares). The opaque triangles show results where the Δ contributions of the model were omitted completely whereas the opaque diamonds represent results of a calculation where only the Δ contributions after pion emission were omitted. In the upper panel the results for the various $|z_\kappa|$ are shown, normalized with respect to our extracted value for $|z_1|$ at 375 MeV, while in the lower panel, the relative deviations of the model calculation from the extracted values are shown.

While a well-founded theoretical interpretation of the obtained partial-wave amplitudes calls for a thorough investigation, e.g. within the framework of effective field theory, as advocated in Refs. [2, 4, 5], the presented analysis allows already to shed light on the role of the Δ (1232) resonance for π^0 production. The importance of the Δ isobar for the reaction $NN \rightarrow NN\pi$ was already pointed out in Ref. [9]. The present partial-wave analysis allows to confirm that aspect nicely in a quantitative and transparent way. The results of the model of Ref. [9, 12] after omitting contributions involving Δ degrees of freedom are shown by the triangles in Fig. 10. The corresponding predictions clearly fall short in describing the amplitudes of the partial-wave analysis. In particular, even the qualitative trend in the magnitude of the amplitude is not reproduced.

Further insight can be gained by taking into account only those $NN \rightarrow N\Delta$ transitions that occur before the pion emission (Fig. 9d and e). The corresponding predictions for the $|z_\kappa|$ are

shown by the open diamonds in Fig. 10. For almost all partial waves this part provides the dominant Δ effect, as expected, since the energy of the incoming NN system is not too far away from the nominal $N\Delta$ threshold. The energy in the outgoing NN system, on the other hand, is much smaller and therefore the excitation of the $\Delta(1232)$ is expected to be of much less significance. However, to achieve also a quantitative agreement with the extracted $|z_\kappa|$, the Δ excitation in the final state (after pion emission: Fig. 9f and g)) is essential, as can be most clearly seen in case of z_2 ($^1S_0 \rightarrow ^3P_0s$) and z_3 ($^1D_2 \rightarrow ^3P_2s$). Especially, only after inclusion of the Δ in the final state the former became larger than the latter.

In this context it is also important to note that both types of contributions, the emission of a real pion from a Δ decay—as depicted in diagrams d) and f) of Fig. 9—and the emission of a virtual pion from a Δ that gets rescattered off the other nucleon—depicted in diagrams e) and g) of Fig. 9—are of similar numerical significance. This should not come as a surprise, for as soon as the Delta-isobar is involved, the large isovector pion nucleon interaction can contribute to the neutral pion production [12]. This is also consistent with the fact that both these contributions (amongst others) contribute at next-to-leading order in the chiral expansion [5].

In any case, it should be clear from this discussion that the Δ degrees of freedom have to be taken into account explicitly in any model that aims at a quantitative description of the reaction $pp \rightarrow pp\pi^0$ even for energies near the pion production threshold.

5 Summary and outlook

We have presented a partial-wave analysis of the double polarization data for the reaction $pp \rightarrow pp\pi^0$, measured at the IUCF [8]. Due to the limited statistical accuracy of the data, following the authors of Ref. [8], we made several assumptions about the contributing amplitudes in order to be able to perform the analysis. The quality of the fit is with a χ^2 per degree of freedom =1.7 not completely satisfying. This could be a consequence of the several assumptions that were made in the analysis.

When compared to the results of a microscopic model [9], the analysis made three important points rather explicit: (i) the Δ degree of freedom is important for a quantitative understanding of the reaction $pp \rightarrow pp\pi^0$, (ii) there is especially one z_κ that very strongly deviates from that extracted from the data, namely z_9 ($^3P_1 \rightarrow ^3P_0p$)—this will guide the search for the possible short-comings of the model, and (iii) the set of partial waves included in the analysis was possibly too limited.

As a next major step a combined analysis of NN scattering data and data on $NN \rightarrow NN\pi$ needs to be performed. On the one hand, the pion production channels provide directly the inelasticities to be used for the analysis of the NN data, on the other hand, the NN elastic phase shifts provide the phase-motion as well as the dominant ϵ dependence of the moduli of the production amplitudes. The latter connection is provided by dispersion integrals as discussed in detail in Refs. [17, 2].

Acknowledgments

We would like to thank Ulf-G. Meißner for a careful reading of the manuscript. We also acknowledge communication with H.O. Meyer and L. Knutson. P.N.D. acknowledges with thanks the support of the Alexander-von-Humboldt Foundation.

References

- [1] P. Moskal *et al.*, Prog. Part. Nucl. Phys. **49**, 1 (2002) [arXiv:hep-ph/0208002].
- [2] C. Hanhart, Phys. Rep. **397**, 155 (2004)[arXiv:hep-ph/0311341].
- [3] V. Bernard, N. Kaiser and U.-G. Meißner, Int. J. Mod. Phys. E **4**, 193 (1995) [arXiv:hep-ph/9501384].
- [4] C. Hanhart, U. van Kolck, and G. Miller, Phys. Rev. Lett. **85**, 2905 (2000) [arXiv:nucl-th/0004033].
- [5] C. Hanhart and N. Kaiser, Phys. Rev. C **66**, 054005 (2002) [arXiv:nucl-th/0208050].
- [6] A. K. Opper *et al.*, Phys. Rev. Lett. **91**, 212302 (2003) [arXiv:nucl-ex/0306027].
- [7] E. J. Stephenson *et al.*, Phys. Rev. Lett. **91**, 142302 (2003) [arXiv:nucl-ex/0305032].
- [8] H. O. Meyer *et al.*, Phys. Rev. C **65**, 027601 (2001).
- [9] C. Hanhart, J. Haidenbauer, O. Krehl and J. Speth, Phys. Lett. B **444**, 25 (1998) [arXiv:nucl-th/9808020].
- [10] Y. Maeda, N. Matsuoka and K. Tamura, Nucl. Phys. **A684**, 392 (2001).
- [11] C. Hanhart, J. Haidenbauer, A. Reuber, C. Schütz and J. Speth, Phys. Lett. B **358**, 21 (1995) [arXiv:nucl-th/9508005].
- [12] C. Hanhart, J. Haidenbauer, O. Krehl and J. Speth, Phys. Rev. C **61**, 064008 (2000) [arXiv:nucl-th/0002025].
- [13] W. W. Daehnick *et al.*, Phys. Rev. C **65**, 024003 (2002) [arXiv:nucl-ex/0108021].
- [14] B. von Przewoski *et al.*, Phys. Rev. C **61**, 064604 (2000) [arXiv:nucl-ex/9912008].
- [15] G. Ramachandran, P. N. Deepak and M. S. Vidya, Phys. Rev. C **62**, 011001(R) (2000).
- [16] G. Ramachandran and M. S. Vidya, Phys. Rev. C **56**, R12 (1997).
- [17] M. Goldberger and K. M. Watson, *Collision Theory* (Wiley, New York, 1964).
- [18] A. H. Rosenfeld, Phys. Rev. **96**, 1 (1954).
- [19] G. A. Miller and P. Sauer, Phys. Rev. C **44**, 1725 (1991).
- [20] K. H. Burrell, Am. J. Phys. **58** (2), 160 (1990).
- [21] P. R. Bevington, *Data Reduction and Error Analysis for the Physical Sciences* (McGraw-Hill, 1969) p 60, Eq. (4-9).
- [22] J. Haidenbauer, K. Holinde and M. B. Johnson, Phys. Rev. C **48**, 2190 (1993).